Fabrication of polyimide bi-stable diaphragms using oxide compressive stresses for the field of 'Buckle MEMS'

2010 J. Micromech. Microeng. 20 075013

(http://iopscience.iop.org/0960-1317/20/7/075013)

J. Micromech. Microeng. **20** (2010) 075013 (6pp) doi:10.1088/0960-1317/20/7/075013

Fabrication of polyimide bi-stable diaphragms using oxide compressive stresses for the field of 'Buckle MEMS'

Usha R Gowrishetty[1], Kevin M Walsh[1] and Thomas A Berfield[2]

[1] Department of Electrical and Computer Engineering, University of Louisville, Louisville, KY, USA
[2] Department of Mechanical Engineering, University of Louisville, Louisville, KY, USA

E-mail: urgowr01@louisville.edu

Received 13 November 2009, in final form 16 April 2010
Published 26 May 2010
Online at stacks.iop.org/JMM/20/075013

Abstract
In this paper we develop vacuum-actuated polyimide bi-stable actuators using buckled diaphragms for applications in the field of MEMS. The fabrication process involves a single mask step and DRIE etch step to fabricate the buckled bi-stable diaphragms. Compressive stresses in a companion thermal oxide layer provide pre-stress in the polyimide mechanical films that initiates diaphragm buckling upon release. Pressure was used to actuate these polyimide diaphragms from their first stable state to their second stable state, resulting in 'zero electrical power' actuation. The buckling height of the polyimide diaphragms is approximately 7.6 μm with an actuation pressure of 41 kPa, which compares favorably with model predictions assuming effective diaphragm properties for a single layer. These polyimide diaphragms can be used as the fundamental building blocks in micro-pumps, micro-valves, switches and optical devices. Because of their bi-stable nature, they can also be used for applications in mechanical memory storage.

(Some figures in this article are in colour only in the electronic version)

1. Introduction

Bi-stable mechanical actuators are of great interest and have begun to appear in the literature in the form of MEMS-based switches [1], micro-valves [2], micro-pumps [3] and mechanical memory devices [4]. Numerous methods for fabricating bi-stable beams [5, 6] and bi-stable diaphragms [7, 8] have been previously reported with electrostatic, pneumatic, magnetic and thermal actuation methods.

Bi-stable actuators possess two stable mechanical equilibrium states, with the transition from the first state to the second state typically in response to an external stimulus (i.e. force, pressure, electric field, vacuum, temperature change, etc). In the case of force, its origin can be electrostatic, magnetic or mechanical. One of the methods to fabricate these bi-stable or quasi bi-stable structures is by engineering compressive stresses in released structures (i.e. beams, diaphragms and cantilevers), resulting in buckling of the micro-structures. More specifically, buckled MEMS-based diaphragms can be formed using microfabricated materials with built-in compressive stresses, as we demonstrate in this paper. Materials such as SiO_2 [9], TiW [10], Cu [11] and Cr [12] are highly compressive depending upon their processing parameters, such as oxidation temperature/time and metal deposition pressure, and are thus viable candidates for MEMS-based bi-stable diaphragms. Such 'buckled MEMS devices' offer two distinct advantages over traditional MEMS actuators—(1) they are capable of much larger displacements, and (2) they can be designed to operate in a true bi-stable mode, similar in operation to an electronic digital circuit.

In this paper we propose a new technique for fabricating bi-stable diaphragms using a combination of polyimide and oxide compressive stresses. The fabricated devices accordingly have two stable states and can be transitioned from one state to another by introducing an external force. In this paper we introduce the external force in the form of a pressure differential across the buckled MEMS diaphragm. Such a device can be used as the building block for a true 'zero power' sensor/switch. These diaphragms can also serve as the

foundation for future generation bi-stable devices in the new field of 'Buckle MEMS'.

The operating principles, design, fabrication and testing of these truly bi-stable devices are as follows.

2. Operating principle and design

Our fabricated buckled diaphragms consist of a polyimide membrane coupled with a thin thermally grown silicon dioxide film. The compressive stresses in the thermal oxide result in buckling of the polyimide membrane. With the application of an actuating pressure, the buckled UP/buckled DOWN diaphragms snap to their respective second state. This threshold value of pressure is referred to as the device's actuation pressure. Upon removal of the actuation force, our devices remain in their second stable state. Buckling and compressive stresses are explained in section 2.1 and our analytical design calculations of the bi-stable diaphragms are presented in section 2.2.

2.1. Buckling and compressive stresses

2.1.1. Buckling due to compressive stresses. Buckling is a mechanical phenomenon that can occur in structures (beams or diaphragms) based on a combination of applied compressive stresses, material stiffness and the slenderness ratio of the structure (radius of gyration/length or thickness/diameter). As lateral compressive loads are applied to a beam or diaphragm, initially the structure is simply compressed. As the compressive stresses are increased further, this compressed state becomes unstable. When the critical buckling stress is reached, the transverse deflection increases rapidly and the beams/diaphragms buckle to their first stable state, which has a lower total strain energy than that of the simple compressed state [8, 13].

2.1.2. Oxide compressive stresses. When silicon is oxidized at high temperatures (e.g. 1000 °C) and cooled, the resulting silicon/silicon dioxide interface is stressed due to the difference in the thermal expansion coefficient of silicon (2.3×10^{-6} K^{-1}) and silicon dioxide (0.5×10^{-6} K^{-1}) [14, 15]. The wet oxide used in our fabrication process was grown at 1000 °C for 1 h on a 4″ n-type silicon wafer and cooled down slowly, resulting in compressive stresses.

Therefore, oxide compressive stresses provide the buckling mechanism for the fabrication of the polyimide/oxide diaphragms in this paper. The polyimide film is essentially stress free as deposited and serves simply as a mechanical layer to provide the necessary structural integrity. Furthermore, the compressive oxide layer is also used as the etch stop for releasing the polyimide/oxide diaphragms.

2.2. Analytical calculations

For our proof-of-concept design, we selected an arbitrary diaphragm diameter of 300 μm, a polyimide thickness of 2.5 μm and an oxide thickness of 0.4 μm. To approximate the switching behavior of the system, a simplistic approach was used in which the bi-layer diaphragm was assumed to act as a single-layer diaphragm with effective mechanical properties. This analysis has a number of limitations and may not be appropriate for all cases. In particular, a more advanced mechanical analysis is required for multilayer systems in which significant residual moments or substrate deformations are present [16]. For the diaphragms fabricated for this study, it was determined that these factors provided negligible contributions to the overall transverse deflections.

The design equations presented in this section are used to predict the diaphragm buckling height, snap height and actuation pressure. The model predictions are then compared with the experimental results in the following section.

The polyimide layer is initially unstressed but undergoes stretching after the release of the diaphragm and large buckling deformation occurs. For simplicity, we use composite rule mixtures theory to calculate an effective Young's modulus for the bi-layer system, where effective in-plane Young's modulus is given by the following equation:

$$E_{\text{eff}} = \frac{\left(d_{\text{SiO}_2} \times E_{\text{SiO}_2} + d_{\text{PI}} \times E_{\text{PI}}\right)}{d_{\text{PI}} + d_{\text{SiO}_2}}, \tag{1}$$

where d_{SiO_2} is the oxide thickness (μm), E_{SiO_2} is Young's modulus of silicon dioxide (73×10^9 Pa) [17], d_{PI} is the polyimide thickness (μm) and E_{PI} is Young's modulus of polyimide (8×10^9 Pa) [17].

Since our diaphragm is composed of a bi-layer film of polyimide and silicon dioxide, we utilized equation (1) and literature-reported material property values for determining the film's effective in-plane Young's modulus. For our diaphragm design with a polyimide (PI-2610) thickness of 2.5 μm and an oxide thickness of 0.4 μm, we obtained an effective Young's modulus of 16.97×10^9 Pa for the bi-layer membrane.

The effective internal stress of the bi-layer film is given by the following equation [18]:

$$\sigma_{\text{film}} = \left(\frac{\sigma_{\text{SiO}_2} \times d_{\text{SiO}_2} + \sigma_{\text{PI}} \times d_{\text{PI}}}{d_{\text{SiO}_2} + d_{\text{PI}}}\right), \tag{2}$$

where σ_{SiO_2} is the stress in the oxide film (MPa) and σ_{PI} is the stress in the polyimide film (MPa).

The polyimide material used in the fabrication of the buckled diaphragm was determined to be stress free when measured using a Toho FLX-2320-S stress measurement system, which fits with the manufacturer's specifications. The stress in the thermally grown wet oxide (0.4 μm) was determined to be −320 MPa using the Toho system. The measured stress values of silicon dioxide and polyimide were used to determine the effective internal stress of the bi-layer diaphragm per equation (2) and this was determined to be −44 MPa. Additionally, the effective stress value of the bi-layer film (silicon dioxide plus polyimide) was experimentally measured using the Toho system and was found to be −44.58 MPa, which is the same as the calculated effective stress value; thus proving that the use of equation (2) is valid in this case. This effective internal stress value was used in our calculations for determining buckling height, snap point buckling height and actuation pressure.

The anticipated buckling height (w_0) of the diaphragm due to the effective stresses in the diaphragm can be calculated using the following equation [7]:

$$W_o = \pm\frac{1}{8}\sqrt{-35\left(\frac{3\sigma_{film}(1-\vartheta^2)R_v^2}{E_{eff}} + 4d^2\right)}, \quad (3)$$

where d is the total diaphragm thickness (μm), R_v is the radius of the diaphragm (μm) and ν is the Poisson's ratio of polyimide (0.2 for PI-2610) [17].

This resulted in a predicted buckling height of 8.6 μm for our design. Furthermore, the height of the buckled diaphragm at the point of snapping or actuation (w_{snap}) is determined to be 5 μm using the equation [7]:

$$W_{snap} = \pm\frac{1}{24}\sqrt{-105\left(3R_v^2\sigma_{film}\frac{(1-\vartheta^2)}{E_{eff}} + 4d^2\right)}. \quad (4)$$

Finally, the actuation pressure (p) required for snapping the diaphragm from its first stable state to its second stable state is determined using equation (5) [7]. For our design the actuation pressure is predicted to be 60 kPa (450 mmHg) of differential pressure:

$$p = \frac{4dw_{snap}}{R_v^2}\left(\frac{4d^2E_{eff}}{3R_v^2(1-\vartheta^2)} + \sigma_{film} + \frac{64w_{snap}^2E_{eff}}{105R_v^2(1-\vartheta^2)}\right). \quad (5)$$

3. Fabrication

We fabricated our devices on (1 0 0) n-type silicon wafers, which were 150 μm in thickness. The wafers were oxidized in a steam oxidation furnace for 1 h resulting in a 0.4 μm thick oxide (figure 1(*a*)). The wafers were then patterned, wet etched in buffer oxide etch (BOE) and DRIEed for about 35 min to etch 120 μm silicon cavities (figure 1(*b*)). Polyimide (PI-2610) was then spun (spread—500 RPM, 2 s, spin—4000 RPM, 20 s) on the other side of the wafer (figure 1(*c*)) and cured overnight on a hotplate at 350 °C. The wafers were then DRIEed to etch the remaining silicon (oxide acts as the DRIE etch stop) and release the polyimide/oxide structures (figure 1(*d*)). Each of the fabricated polyimide/oxide diaphragms (300 μm diameter) was buckled either UP or DOWN due to the compressive stresses in the oxide with a buckling height ranging between 7 and 9 μm. The direction of the buckling phenomena appeared random. This is markedly different from other reports in the literature in which the diaphragms buckle preferentially toward the oxide [8]. The random nature of our diaphragm's buckling direction was the first indication of our device's true bi-stability, unlike other buckled diaphragms reported in the literature. The randomness of the initial buckling direction also indicates that the effects of residual moments may be neglected. A significant residual moment would induce a transverse deflection in the diaphragm and bias the initial buckling direction.

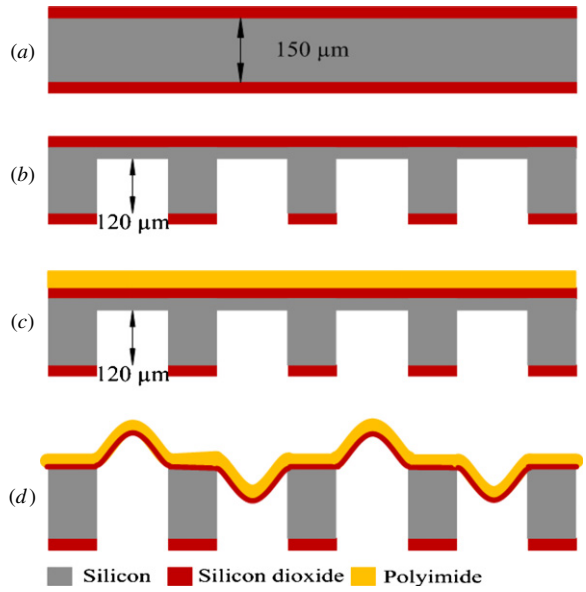

Figure 1. (*a*) 300 μm thick DSP wafer wet-oxidized resulting in 0.4 μm thick silicon dioxide. (*b*) Wafer patterned with 300 μm diameter holes and DRIEed to etch 120 μm silicon. (*c*) PI-2610 is spin-coated on the DRIEed wafer. (*d*) PI+oxide diaphragms are released by etching away (i.e. DRIE) the remaining silicon. Resulting diaphragms are either buckled UP or DOWN because of the compressive stresses in the oxide.

4. Testing and experimental results

For testing, the released diaphragms were first pressurized from the wafer backside so that all the diaphragms initially started in their buckled UP state. The initial buckle height was measured and then vacuum was applied on individual diaphragms to test their bi-stability, actuation pressure and snap height. The test set-up consisted of a micromachined chuck for holding the die, a vacuum pump, a regulator and a Dektak contact profilometer for surface profiling. Care was taken to experimentally verify that the contact pressure exerted by the Dektak stylus did not affect the diaphragm deflection measurements. We experimentally determined that for a Dektak stylus force of below 2 mg, there was no measurable adverse effect on the diaphragm deflection. Accordingly, a stylus force of 1 mg was used for all the profilometry measurements.

Figures 2(*a*) and (*b*) show the surface profile of one of the as-fabricated buckled UP diaphragms in its first state with no external pressure applied to it. Its initial buckling height was measured to be approximately −7.6 μm (see figure 5(*b*) for direction polarity). We then applied pressure to the diaphragm to switch it to its second state. Figures 3(*a*) and (*b*) show the surface profile of the buckled DOWN diaphragm in its second state with pressure once again removed. The buckling height of the diaphragm in its second state was measured to be approximately 7.8 μm. The inset in figures 2(*b*) and 3(*b*) show an optical image of the buckled diaphragm using the DIC (differential interference contrast) feature of a Nikon microscope. As the diaphragm flips to its complementary

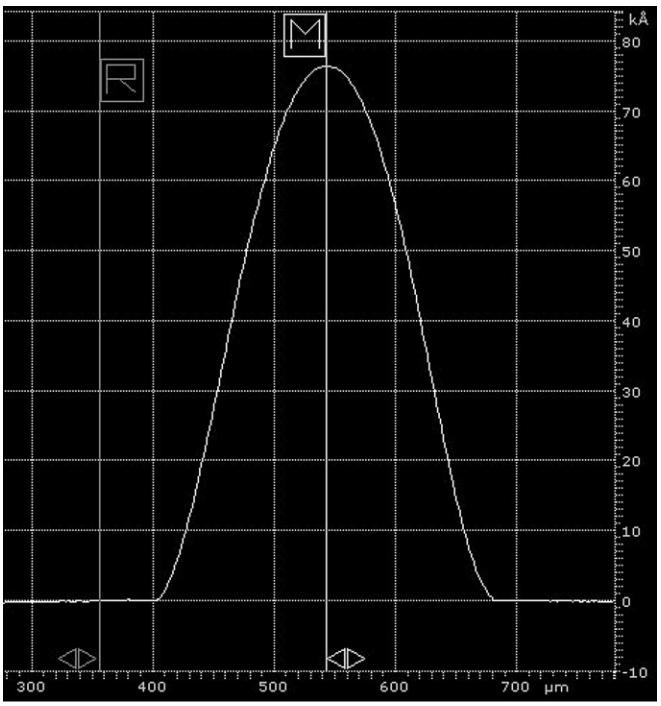

(*a*)

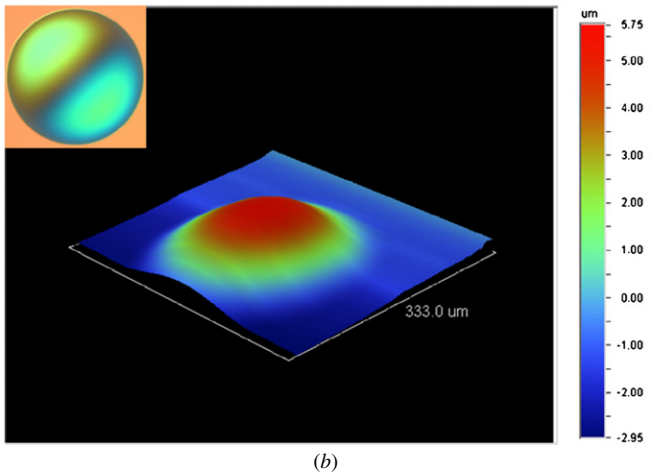

(*b*)

Figure 2. (*a*) Contact profile of the first state of the 300 μm diameter buckled PI+oxide diaphragm (7.6 μm buckling height). (*b*) 3D profile of the first state of a 300 μm PI+oxide diaphragm (inset—optical image of the first state of the diaphragm using DIC).

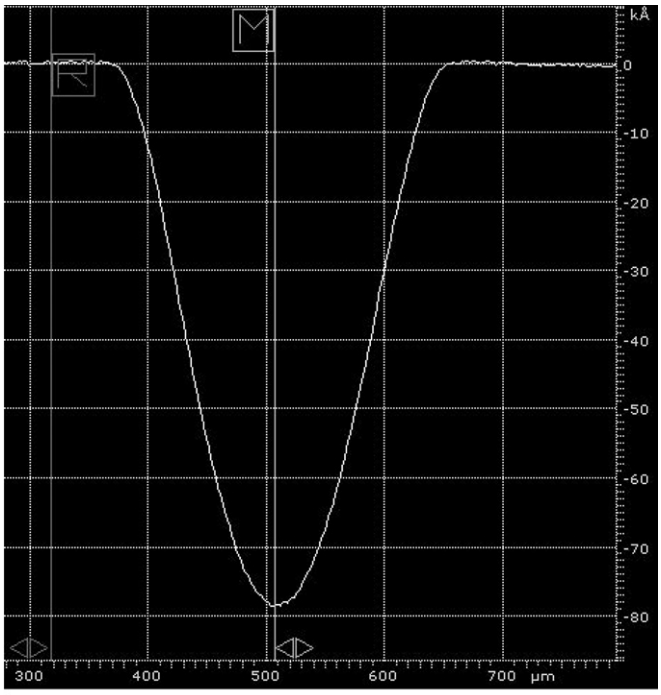

(*a*)

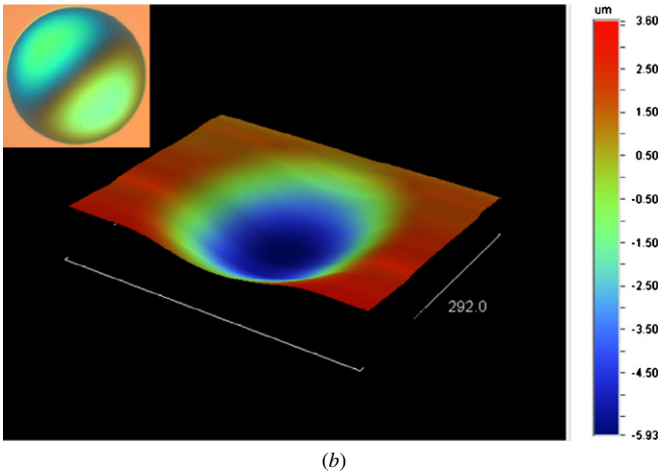

(*b*)

Figure 3. (*a*) 3D profile of the second state of 300 μm diameter PI+oxide diaphragm (7.86 μm buckling height). (*b*) 3D profile of the second state of 300 μm PI+oxide diaphragm (inset—optical image of second state of the diaphragm using DIC).

stable state, one can observe an interesting change in the color pattern of the image, as seen in the insets.

The diaphragm was then switched back to its buckled UP state and then slowly vacuum-actuated from its backside in steps of 50 and 20 mmHg (6.6 and 2.6 kPa) to determine exactly when it switches. Simultaneously, the shape and height of the diaphragm was measured using the Dektak profiler. Figure 4 shows a plot of buckling height varying with pressure and the buckled diaphragm in its first and second state. Figure 4(*a*) shows our experimental results (square markers), as well as the theoretical prediction (solid line) using equation (5). The displacement data were measured at the center of the diaphragm. As shown in figure 4(*a*), starting from the left side of the graph, the buckled diaphragm starts out with an initial height of -7.6 μm. As pressure is slowly applied, the height of the diaphragm gradually decreases until it eventually snaps to its second buckled DOWN state. This occurred experimentally at 41 kPa or 305 mmHg. With pressure still applied, the buckled diaphragm deforms to a displacement of 9.1 μm (rightmost data point in figure 4(*a*)). Upon release of the actuation pressure, the buckled diaphragm relaxes back to a final displacement value of 7.8 μm. It is interesting to note that the rest values of the buckling height of the diaphragm in its buckled UP and buckled DOWN states are approximately equal and opposite, another indicator of the negligible residual film strain gradient.

Table 1. Comparison of theoretical calculations with experimental results.

	Theoretical calculations	Experimental results
Dimensions	$R = 150\ \mu$m $d_{\text{total}} = 2.9\ \mu$m $d_{SiO_2} = 0.4\ \mu$m $d_{PI} = 2.5\ \mu$m	$R = 150\ \mu$m $d_{\text{total}} = 2.9\ \mu$m $d_{SiO_2} = 0.4\ \mu$m $d_{PI} = 2.5\ \mu$m
Assumptions	$E_{PI} = 8 \times 10^9$ Pa $E_{SiO_2} = 73 \times 10^9$ Pa $\nu = 0.2$ Stress $= -320$ MPa (silicon dioxide stress measured using Toho)	NA
Buckling height (μm)	8.6	7.6
Buckling height @ snap point (μm)	5	6.3
Actuation pressure (kPa)	60	41

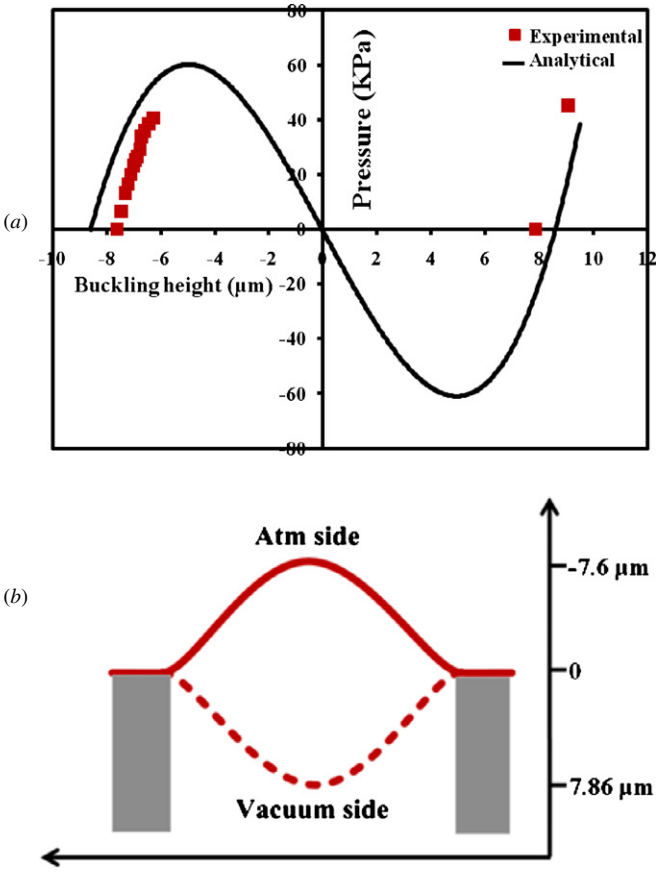

Figure 4. (*a*) Buckled UP (first state) diaphragm snapping DOWN (second state) at an actuating pressure of 41 kPa or 305 mmHg. Buckling height was measured using a contact profilometer for varying pressures (square markers—experimental data, solid line—theoretical data using equation (5)). (*b*) Buckled diaphragm in the first (UP) and second (DOWN) state.

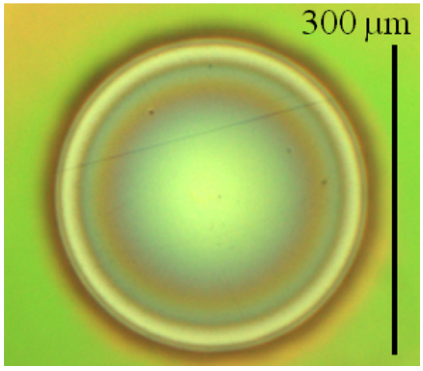

Figure 5. Optical image of concentric oxide circles resulting from the partially etched oxide during the second DRIE step. Shown here is the reverse side of the buckled oxide/PI diaphragm.

5. Discussions and applications

The theoretical curve in figure 4(*a*) was determined using equation (5). The stress value of the bi-layer film used for analytical calculations was determined using a Toho stress measurement system as mentioned earlier. All the remaining material parameters were assumed from the literature (Poisson's ratio and Young's modulus), and all specimen dimensions were measured directly (diaphragm diameter and thickness). The experimental measurements of the bi-layer diaphragm match the analytical profile reasonably well. Deviations can be attributed to the inherent non-uniformity of the thickness and stress of the micromachined PI/oxide diaphragm due to the DRIE etching process. As shown in figure 4(*a*), the theoretical actuation pressure was predicted to be 60 kPa (450 mmHg) compared with the experimental actuation pressure of 41 kPa (305 mmHg). Furthermore, the theoretical buckling height actuation or the snap point was predicted to be 5 μm as compared with the experimental value of 6.3 μm.

Table 1 summarizes the comparison of the experimental results of our device with our theoretical calculations. The data presented in table 1 are representative of the majority of the 300 μm diaphragms fabricated on the silicon wafer. The calculated actuation pressure, buckling height at snap point and buckling height were moderately different from the experimental values. This can be explained by the fact that our micromachined bi-layer diaphragms are slightly non-uniform due the DRIE etching process. The theory presented in section 2 assumes uniform and constant values of all of the diaphragm parameters. With micromachined bi-layer diaphragms, this is difficult to control. For example, during the DRIE release step of the diaphragms, oxide is partially etched around the edges of the diaphragm. The partially etched oxide, which appears as concentric circles under an optical

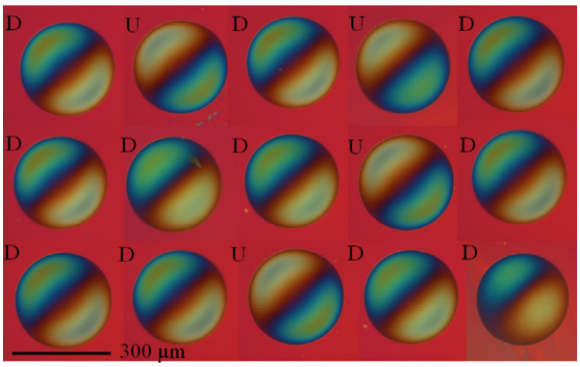

Figure 6. Optical image (using DIC) of buckled UP (U) and buckled DOWN (D) diaphragms (300 μm diameter) for application as mechanical memory storage devices.

microscope (see figure 5), results in slight deviations in the oxide thickness near the diaphragm edges and non-uniform compressive stresses over the 300 μm diameter diaphragms. This can be a source of error with our modeling equations as it directly affects the average internal stress value.

One of the applications of buckled diaphragms is in mechanical memory storage devices. An optical image of a set of buckled polyimide + oxide diaphragms is shown in figure 6. The diaphragms are randomly buckled UP or DOWN during the diaphragm release step. The diaphragms can be easily modified using pressure to change the buckling orientation, and thus can be used as a mechanical storage device. Some of the other applications of these buckled diaphragms are in micro-pumps, micro-valves, optical lenses and switches.

6. Conclusions

We successfully designed, fabricated and tested MEMS-based polyimide/oxide membranes with engineered oxide compressive stresses resulting in three-dimensional buckled diaphragms. The 300 μm diameter micromachined structures were pressure tested and determined to be truly bi-stable. We experimentally measured a buckling height of 7.6 μm and an actuation pressure of 41 kPa for our bi-layer diaphragms, which compared favorably to our modeling predictions. We also report experimental pressure-displacement data on these MEMS-based bi-stable circular diaphragms. Applications for these three-dimensional actuators include no-power sensors, micro-pumps, micro-valves, programmable switches, mechanical memory and optical devices.

Acknowledgments

The effort was funded by the US Navy under contract DAAB07-03-D-B010/TO-0198. Technical program oversight under the Navy contract was provided by the Naval Surface Warfare Center, Crane Division. The authors would also like to thank Dr Julia Aebersold of University of Louisville for her technical support with polyimide processing.

References

[1] Huff M A, Nikolich A D and Schmidt M A 1991 A threshold pressure switch utilizing plastic deformation of silicon *Proc. Int. Conf. Solid-State Sensors Actuators (Transducers'91)* pp 177–80
[2] Popescu D S *et al* 1995 Silicon active microvalves using buckled membranes for actuation *Proc. Int. Conf. Solid-State Sensors Actuators (Transducers'95)* pp 305–8
[3] Nisar A *et al* 2008 MEMS-based micropumps in drug delivery and biomedical applications *Sensors Actuators* B **130** 917–42
[4] Halg B 1990 On a micro-electro-mechanical nonvolatile memory cell *IEEE Trans. Electron Devices* **37** 7
[5] Vangbo M and Backlund Y 1998 A lateral symmetrically bistable buckled beam *J. Micromech. Microeng.* **8** 29
[6] Jin Q, Lang J H and Slocum A H 2004 A curved-beam bistable mechanism *J. Microelectromech. Syst.* **13** 137–46
[7] Schomburg W K and Goll C 1998 Design optimization of bistable microdiaphragm valves *Sensors Actuators* A **64** 259–64
[8] Arya R *et al* 2006 Thermally actuated, bistable, oxide/silicon/metal membranes *J. Micromech. Microeng.* **16** 40
[9] EerNisse E P 1979 Stress in thermal SiO_2 during growth *Appl. Phys. Lett.* **35** 8–10
[10] O'Donnell K, Kostetsky J and Post R S 2002 Stress control in NiV, Cr and TiW thin films used in UBM and backside metallization. Paper presented at *Flip Chip Technology Conference (Austin, Texas, 2002)*
[11] Pletea M *et al* 2005 Stress evolution during and after sputter deposition of Cu thin films onto Si (1 0 0) substrates under various sputtering pressures *J. Appl. Phys.* **97** 054908
[12] Janssen G C A M and Kamminga J-D 2004 Stress in hard metal films *Appl. Phys. Lett.* **85** 3086–8
[13] Ding X *et al* 1990 A study on silicon-diaphragm buckling *Tech. Dig. IEEE Solid-State Sensors and Actuators Workshop (Hilton Head Island, SC, USA 1990)* pp 128–31
[14] Miura H, Sakata H and Sakata S 1993 Residual stress measurement in silion substrate after local thermal oxidation using microscopic Raman spectroscopy *JSME Int. J. Ser. A (Mechanics and Material Engineering)* **36**-A(3) 302–8
[15] http://www.flipchips.com/tutorial22.html
[16] Wang X, Li J and Zhang T-Y 2006 Microbridge tests: I. On asymmetrical trilayer films *J. Micromech. Microeng.* **16** 122–33
[17] Ozsun O *et al* 2009 On heat transfer at microscale with implications for microactuator design *J. Micromech. Microeng.* **19** 045020
[18] Zohni O *et al* 2007 Investigating thin film stresses in stacked silicon dioxide/silicon nitride structures and quantifying their effects on frequency response *J. Micromech. Microeng.* **17** 1042